Articles

Experimental Tests for Protrusion and Undulation Pressures in Phospholipid Bilayers†

T. J. McIntosh,*,‡ S. Advani,‡ R. E. Burton,‡ D. V. Zhelev,§ D. Needham,§ and S. A. Simon‖

Departments of Cell Biology, Neurobiology, and Anesthesiology, Duke University Medical Center, Durham, North Carolina 27710, and Department of Mechanical Engineering and Materials Science, Duke University, Durham, North Carolina 27706

Received February 17, 1995; Revised Manuscript Received May 5, 1995⊗

ABSTRACT: Theoretical treatments predict that strong entropic pressures between adjacent bilayer membranes can arise from out of plane motions caused by either thermally induced bending undulations of the entire bilayer [Harbich, W., & Helfrich, W. (1984) *Chem. Phys. Lipids 36*, 39−63; Evans, E. A., & Parsegian, V. A. (1986) *Proc. Natl. Acad. Sci. U.S.A. 83*, 7132−7136] or protrusions of individual lipid molecules from the bilayer surface [Israelachvili, J. N., & Wennerström, H. (1992) *J. Phys. Chem. 96*, 520−531]. To determine the relative contributions of these motions to the repulsive pressure between phospholipid bilayers, the osmotic stress/X-ray diffraction method was used to measure the range and magnitude of the total repulsive pressure, and micropipet methods were used to measure the bending moduli of phosphatidylcholine bilayers containing lysophosphatidylcholine and polyunsaturated diarachidonoylphosphatidylcholine (DAPC) bilayers. In the gel phase, incorporation of equimolar lysophosphatidylcholine into phosphatidylcholine bilayers caused the hydrocarbon chains from apposing monolayers to interdigitate, but did not appreciably change the equilibrium fluid spacing in excess buffer from its control value of 12 Å. In contrast, the incorporation of equimolar lysophosphatidylcholine into liquid-crystalline phase phosphatidylcholine bilayers markedly increased the range of the repulsive pressure so that equilibrium fluid separation increased from 15 to 28 Å, and also decreased the bilayer bending modulus from 5.1×10^{-13} to 1.3×10^{-13} erg. Liquid-crystalline DAPC bilayers had intermediate values of both equilibrium fluid separation (20 Å) and bending modulus (2.8×10^{-13} erg). Analysis of these data indicates that (1) the relative importance of entropic pressures compared to the hydration pressure depends strongly on the composition and structure of the bilayer, (2) the protrusion pressure may contribute to the total repulsive pressure at large pressures or small fluid spacings, and (3) the repulsive undulation pressure, together with the attractive van der Waals pressure, is a primary factor in determining the fluid spacing at low and/or zero applied pressures in liquid-crystalline bilayers.

A strong, short-ranged repulsive interaction has been shown to exist between electrically neutral phospholipid bilayers (LeNeveu et al., 1977; Parsegian et al., 1979; McIntosh & Simon, 1986, 1993; Rand & Parsegian, 1989). This interaction is thought to contain a number of components, including a hydration (solvation) pressure, arising from the ordering of water molecules by the hydrophilic bilayer surface (Marcelja & Radic, 1976; Parsegian et al., 1979; Cevc & Marsh, 1985; McIntosh & Simon, 1986; Rand & Parsegian, 1989; Leikin et al., 1993), and entropic (steric) pressures, arising from contact between phospholipid molecules from apposing bilayers (Helfrich, 1978; McIntosh et al., 1987, 1989a; Israelachvili & Wennerström, 1990, 1992; McIntosh & Simon, 1994).

Among the entropic pressures either shown or postulated to exist between liquid-crystalline phosphatidylcholine bilayers are (1) a very short-range (≤5 Å) pressure due to the motion of phospholipid head groups (McIntosh et al., 1987, 1989a; McIntosh & Simon, 1993), (2) an undulation or fluctuation pressure, due to thermally driven undulations or flucutations of the entire bilayer surface (Helfrich, 1978; Evans & Parsegian, 1986; Evans, 1991), and (3) a protrusion pressure, due to "fingerlike" protrusions or excursions of individual lipid molecules into the fluid space between bilayers (Israelachvili & Wennerström, 1990, 1992). A brief summary of the theoretical or experimental bases for each of these pressures is presented below.

In terms of the first, very short range pressure, an upward break in pressure−distance relations at a fluid spacing of

† This work was supported by a grant from the National Institutes of Health (GM-27278).

‡ Department of Cell Biology, Duke University Medical Center.

§ Department of Mechanical Engineering and Materials Science, Duke University.

‖ Departments of Neurobiology and Anesthesiology, Duke University Medical Center.

⊗ Abstract published in *Advance ACS Abstracts,* June 15, 1995.

0006-2960/95/0434-8520$09.00/0

4−5 Å has been observed for phosphatidylcholine bilayers (McIntosh et al., 1989a). The range of this pressure and the observations that it is a strong function of both the density of head groups at the bilayer/water interface (McIntosh & Simon, 1994) and the motion of the head groups (McIntosh & Simon, 1993) are consistent with this pressure being due to the steric interaction between head groups from apposing bilayers. At present there are no rigorous theoretical treatments of this pressure.

The undulation pressure was first postulated by Helfrich (1978), on the basis of observations of the disjoining of fully hydrated liposomes. Several theoretical treatments (Helfrich, 1978; Harbich & Helfrich, 1984; Evans & Parsegian, 1986; Evans & Ipsen, 1991; Podgornik & Parsegian, 1992) have predicted that the magnitude of the undulation pressure should depend on the bending modulus of the bilayer. Experimentally, the presence of membrane undulations has been demonstrated by micropipet manipulations of large vesicles (Evans & Rawicz, 1990), neutron spin echo studies of phosphatidylcholine (PC)[1] multilayers (Pfeiffer et al., 1993), analyses of X-ray diffraction patterns of micelles (Safinya et al., 1986, 1989; Roux & Safinya, 1988), and analysis of the amplitudes and harmonics of vesicle contours (Faucon et al., 1989). Pressure−distance relations for solid and fluid monoglyceride bilayers have shown the contribution of undulations to the repulsive interactions for liquid-crystalline bilayers (McIntosh et al., 1989c). However, in the case of phospholipid bilayers there is little direct experimental data concerning the relative contribution of the undulation pressure to the total pressure.

The protrusion pressure has been postulated by Israelachvili and Wennerström (1990, 1992) who theorized that molecular scale protrusions of the "hydrocarbon chains and other parts of the molecules" from the lipid surface would give rise to a strong, short-range repulsive pressure between apposing bilayers. Experimental data have indicated the presence of molecular protrusions in liquid-crystalline lipid bilayers. Incoherent quasielastic neutron scattering studies of phosphatidylcholine multilayers revealed molecular protrusions of amplitudes 0.5 Å at 10^{12} Hz and 2.5 Å at 10^{10} Hz (Pfeiffer et al., 1989; Konig et al., 1992), although subsequent analyses indicated that the slower motion may be associated with undulations rather than protrusions (Pfeiffer et al., 1993). Phospholipid exchange between large unilamellar vesicles occurs via the diffusion through the aqueous phase of monomers of diacyl lipids (MacDonald, 1985; Wimley & Thompson, 1991; Wu & Lentz, 1991). In addition, computer simulations of hydrated bilayers have shown that individual lipid molecules protrude, to various extents, from the bilayer (Heller et al., 1993; Marrink et al., 1993; Damodaran & Merz, 1994). A question regarding the validity of the protrusion model is that it does not seem to explain the relatively large fluid spacing observed between gel-phase bilayers, where protrusions would be expected to be very small or absent (Parsegian & Rand, 1991; McIntosh & Simon, 1993, 1994). Moreover, the protrusion model has been challenged on theoretical grounds for liquid-crystalline bilayers (Parsegian & Rand, 1991, 1992). One of the key issues has been the relative magnitude of lipid solubilities predicted by the protrusion model and experimentally measured critical micelle concentrations of phospholipid molecules with two hydrocarbon chains (Israelachvili, 1992; Parsegian & Rand, 1992). At this time there are no pressure−distance measurements providing the magnitude of the protrusion pressure relative to other repulsive pressures.

A basic difference between molecular protrusions and bilayer undulations is in the number of molecules involved, one in the case of protrusions and many thousands in the case of undulations. However, it is also possible that protrusions involving several molecules might contribute to the repulsive pressure. Lipowsky and Grotehans (1993, 1994) have presented a model for the interactions between fluid bilayers which contains a short-range repulsive pressure (assumed to arise from the hydration pressure) and thermally excited protrusions that arise from correlated displacements of several molecules, rather than single molecules as in the Israelachvili and Wennerström (1990, 1992) protrusion model.

To shed light on the relative contributions of bilayer undulations and molecular protrusions to the total repulsive pressure between phospholipid bilayers, in this paper we measure pressure−distance relations for phospholipid bilayers that should exhibit a range of bending moduli and a range of protrusions of individual lipid molecules. These bilayers include polyunsaturated diarachidonoylphosphatidylcholine (DAPC) bilayers, and both gel and liquid-crystalline phosphatidylcholine (PC) bilayers containing large (equimolar) concentrations of monoacyl phosphatidylcholine (lysophosphatidylcholine). Compared to well-characterized egg phosphatidylcholine bilayers, DAPC bilayers have a smaller bending modulus (Evans & Rawicz, 1990), whereas gel-phase PC bilayers are much less compressible (Needham & Nunn, 1990), thus making them much more difficult to bend. Comparisons of pressure−distance relations for diacyl phosphatidylcholine bilayers in the presence and absence of monoacyl phosphatidylcholine should provide an experimental test for the protrusion model because (1) the theoretical treatment (Israelachvili & Wennerström, 1990, 1992) predicts that the decay length of the protrusion pressure should be inversely proportional to the lateral dimensions of the protruding molecule, and monoacyl phosphatidylcholines have smaller lateral dimensions than diacyl phospholipids; (2) lysophosphatidylcholines have critical micelle concentrations several orders of magnitude larger than diacyl phosphatidylcholines (Marsh, 1990); and (3) rate constants of lysophosphatidylcholine adsorption from the aqueous phase into unilamellar PC vesicles and desorption from unilamellar PC vesicles to the aqueous phase (Elamrani & Blume, 1982; Needham & Zhelev, 1995) indicate that lysophosphatidylcholine can partition out of a vesicle into the aqueous phase. Previous studies (Van Echteld et al., 1981) have shown that large concentrations (up to 50 mol %) of lysophosphatidylcholines can be incorporated into both gel and liquid-crystalline phase phosphatidylcholine bilayers. Since lysophosphatidylcholine has the same polar head group as diacyl phosphatidylcholine, incorporation of lysophosphatidylcholine should have little effect on the hydration pressure of diacyl phosphatidylcholine bilayers. Moreover, since the magnitude of the hydration pressure has been shown

[1] Abbreviations: PC, phosphatidylcholine; EPC, egg phosphatidylcholine, DPPC, dipalmitoylphosphatidylcholine; MOPC, monooleoylphosphatidylcholine; MPPC, monopalmitoylphosphatidylcholine; DOPE, dioleoylphosphatidylethanolamine; DAPC, diarachidonoylphosphatidylcholine; PVP, poly(vinylpyrrolidone).

to be proportional to the square of the measured dipole potential (Simon & McIntosh, 1989), information on the effects of lysophosphatidylcholine on the hydration pressure can be obtained from measurements of the dipole potential in the presence and absence of lysophosphatidylcholine. Since the fluctuation pressure depends on the bilayer bending modulus (Helfrich, 1978; Evans & Parsegian, 1986; Evans, 1991), measurements of the bending modulus are also made for all these bilayer systems.

MATERIALS AND METHODS

Materials

Egg phosphatidylcholine (EPC), dipalmitoylphosphatidylcholine (DPPC), monopalmitoylphosphatidylcholine (MPPC), monooleoylphosphatidylcholine (MOPC), and rhodamine-labeled dioleoylphosphatidylethanolamine (DOPE-rhodamine) were obtained from Avanti Polar Lipids, Inc. (Alabaster, AL). Dextran with an average molecular mass of 503 000 Da and poly(vinylpyrrolidione) (PVP) with an average molecular mass of 40 000 Da were purchased from Sigma Chemical Co. (St. Louis, MO).

Methods

X-ray Diffraction/Osmotic Stress. Two types of multibilayer systems were examined by X-ray diffraction, unoriented suspensions of multiwalled vesicles and oriented multilayers. Known osmotic pressures were applied to each of these systems by published procedures (LeNeveu et al., 1977; Parsegian et al., 1979; McIntosh & Simon, 1986; McIntosh et al., 1987). Osmotic stress was applied to the liposomes by incubating them in aqueous solutions of the neutral polymers dextran and PVP. Since these polymers are too large to enter the lipid lattice, they compete for water with the lipid multilayers, thereby applying an osmotic pressure (LeNeveu et al., 1977; Parsegian et al., 1979). Osmotic pressures for dextran and PVP solutions have been published (Parsegian et al., 1986; McIntosh et al., 1989b). Pressure was applied to oriented multibilayers by incubating them in constant relative humidity atmospheres maintained with saturated salt solutions. The ratio of the vapor pressure (p) of various salt solutions to the vapor pressure of pure water (p_o) has been determined (O'Brien, 1948; Weast, 1984). The applied pressure is given by

$$P = -(RT/V_w) \ln(p/p_o) \quad (1)$$

where R is the molar gas constant, T is the temperature in degrees Kelvin, and V_w is the partial molar volume of water (Parsegian et al., 1979).

Unoriented suspensions of EPC:MOPC or DPPC:MPPC bilayers were made by codissolving the appropriate lipids in chloroform, removing the chloroform under vacuum, adding excess water or polymer solution, and incubating with extensive vortexing above the lipid's phase transition temperature. Suspensions of DAPC were made by a similar procedure with a couple of modifications. To avoid lipid oxidation, most DAPC samples were made by adding lyophilized lipid to polymer solutions made with a buffer containing 100 mM NaCl, 20 mM HEPES, and 10 mM ascorbic acid at pH 7. To ensure equilibration of the salt across the multilayers, several freeze−thaw cycles were used. In control experiments, similar X-ray results were obtained for specimens made in either excess buffer or excess water for either EPC:MOPC bilayers or DAPC bilayers. All suspensions were pelleted with a bench centrifuge, sealed in quartz glass X-ray capillary tubes, and mounted in a point collimation X-ray camera.

Oriented multilayers of DAPC or EPC:MOPC were formed by placing a small drop of lipid in chloroform solution onto a curved glass substrate and evaporating the chloroform under a gentle stream of nitrogen. The multilayers on the glass substrate were mounted in a controlled humidity chamber on a single-mirror (line-focused) X-ray camera such that the X-ray beam was oriented at a grazing angle relative to the multilayers (McIntosh et al., 1987, 1989b). The humidity chamber, which contained a cup of the appropriate saturated salt solution, consisted of a hollow-walled copper cannister with two Mylar windows for passage of the X-ray beam. To speed equilibration, a gentle stream of nitrogen was passed through a flask of the saturated salt solution and then through the chamber.

For both oriented and unoriented specimens, X-ray diffraction patterns were recorded on Kodak DEF X-ray film at room temperature (21 ± 2 °C). X-ray films were processed by standard techniques and densitometered with a Joyce-Loebl microdensitometer as described previously (McIntosh & Simon, 1986; McIntosh et al., 1987, 1989b). After background subtraction, integrated intensities, $I(h)$, were obtained for each order h by measuring the area under each diffraction peak. For unoriented patterns, the structure amplitude $F(h)$ was set equal to $\{h^2I(h)\}^{1/2}$ (Blaurock & Worthington, 1966; Herbette et al., 1977). For the oriented line-focused patterns the intensities were corrected by a single factor of h due to the cylindrical curvature of the multilayers (Blaurock & Worthington, 1966; Herbette et al., 1977) so that $F(h) = \{hI(h)\}^{1/2}$.

Electron density profiles, $\varrho(x)$, on a relative electron density scale were calculated from

$$\varrho(x) = (2/d) \sum \exp\{i\phi(h)\}F(h) \cos(2\pi xh/d) \quad (2)$$

where x is the distance from the center of the bilayer, d is the lamellar repeat period, $\phi(h)$ is the phase angle for order h, and the sum is over h. Phase angles were determined by the use of continuous Fourier transforms calculated with the sampling theorem (Shannon, 1949), as described in detail previously (McIntosh & Holloway, 1987; McIntosh et al., 1989a). Electron density profiles described in this paper are at a resolution of $d/2h_{max} \approx 7$ Å.

Bending Modulus Measurements. The area expansion and bending moduli were measured by performing micropipet mechanical tests that were initially developed by Evans and co-workers (Kwok & Evans, 1981; Evans & Rawicz, 1990) and later modified by Zhelev et al. (1994). Briefly, the vesicles were observed either by bright field or by epifluorescence microscopy in an inverted Leitz microscope with a 100× oil immersion objective. The microscope images were recorded using a Hamamatsu CCD (for bright field) or Hamamatsu SIT (for epifluorescence) camera. The experimental chamber was 3 mm thick and open on both sides for micromanipulation. The temperature of the chamber was kept at 14 °C by a flow of thermostated water between two glass slides on the top of the chamber. Micropipets were made from 0.75-mm capillary glass tubing pulled to a fine

point with a vertical pipet puller and cut at the desired diameter (~5 μm) using a microforge. In order to "passivate" the glass surface of the pipet tip, it is usual to include a small amount of albumin (0.1 g %) in the working solutions. However, since albumin has a strong interaction with lysolipids, albumin was excluded from working solutions and the pipets were prepassivated by incubation for 1 h in 170 mosm glucose with 0.5% bovine serum albumin. This albuin coat remained on the micropipet surface during the course of the experiments. The pipet was connected to a manometer system so that the pipet suction pressure could be varied between 0.5 and 100 Pa using the micrometer-driven displacement of a water reservoir. These low suction pressures were measured by a differential pressure transducer (Validyne DP103). Higher pressures up to 10 000 Pa were measured with a second pressure transducer (Validyne P7D). Readouts from the pressure transducers were displayed on the video image using a video multiplexer (Vista Electronics 401).

Lipid vesicles composed of either EPC, 1:1:0.001 EPC:MOPC:DOPE-rhodamine, or 1:0.001 DAPC:DOPE-rhodamine were prepared by dissolving the lipid or lipid mixtures in chloroform at 10 mg/mL. DOPE-rhodamine was added so that the vesicles could be observed with the fluorescence microscope and unilamellar vesicles could be distinguished from those containing two or more bilayers. Control experiments, performed in the absence of DOPE-rhodamine, showed that these low concentrations of DOPE-rhodamine did not affect the bilayer bending modulus measurements. One hundred microliters of this solution was dried under nitrogen onto a roughened Teflon sheet (Needham & Evans, 1988). The dried lipid was allowed to swell overnight in 2 mL of 166 mosm sucrose solution, so that the vesicles had sucrose solution in their interior. (In the case of DAPC vesicles, this swelling procedure was performed under nitrogen in order to reduce the tendency for C=C bond hydrolysis). The vesicles were then suspended in glucose solutions to improve optical contrast and for ease of capture (Needham & Evans, 1988). It was important, especially for the EPC:MOPC vesicles, to provide experimental conditions in which the vesicle membrane and the glucose bathing medium were at equilibrium with respect to the soluble MOPC. To do this, a glucose solution containing the same amount of lipid monomers and/or micelles as the vesicle-containing solution was used as the bathing solution in all micropipet experiments. That is, after incubation in a glucose solution, the lipid suspension was centrifuged, and the supernatant was used as bathing solution in the micropipet experiments.

The bending modulus was found from the measured change in projected area of the vesicle for a series of increasing membrane tensions. The area change (α) was found from the measured projection length inside the pipet, assuming that the volume of the vesicle was preserved (Kwok & Evans, 1981). The membrane tension (τ) was determined from the pipet suction pressure (ΔP) and pipet and vesicle geometry by the relation (Evans & Skalak, 1980; Kwok & Evans, 1981)

$$\Delta P = 2\tau\{1/R_p - 1/R_{out}\} \quad (3)$$

where R_p is the pipet radius and R_{out} is the radius of the vesicle outside the pipet.

In order to carry out these experiments, the vesicles must have a slight excess of membrane area compared to a sphere of the same volume. To produce this excess area, the vesicles were slightly deflated by using a bathing solution that had a slightly higher osmolarity than the sucrose solution inside the vesicles. Under these conditions the vesicle membrane is subjected to thermal undulations. Then, when a tension is applied to the vesicle membrane (by increasing the applied micropipet suction pressure), its apparent area increases, as measured by the increase in the projection length of the membrane in the micropipet. As discussed by Evans and Rawicz (1990), this increase in apparent vesicle area (α) is the sum of two components: one due to a decrease in the amplitude of membrane undulations and the other due to the direct expansion of the area per molecule of the membrane itself. At low tensions (<0.5 dyn/cm) the area change is determined primarily by thermal undulations, and the slope of $\ln(\tau)$ versus α is proportional to the elastic bending modulus, k_c. That is, the bending modulus can be obtained from the relation

$$k_c \approx mKT/8\pi \quad (4)$$

where m the is slope of $\ln(\tau)$ versus α at low tensions (Evans & Rawicz, 1990). The elastic area expansion modulus, K_a, can be obtained from the slope of τ versus α at high tensions (Evans & Rawicz, 1990), since in the high-tension regime

$$K_a \approx \tau/\alpha \quad (5)$$

Dipole Potential Measurements. Dipole potentials, V, were measured as described previously (MacDonald & Simon, 1987). Monolayers of DAPC or 1:1 EPC:MOPC were formed by spreading 10 μL of a 10 mg/mL lipid in hexane:ethanol (9:1, v/v) solution onto a subphase of 0.1 M KCl (the KCl was previously roasted at 600 °C) in a trough having a surface area of about 70 cm^2. Under these conditions it has been shown that the packing of the lipid molecules in the monolayer is approximtely the same as it is in a bilayer (MacDonald & Simon, 1987). The dipole potential was measured at room temperature between a Ag/AgCl electrode in the subphase and a ^{241}Am electrode in air using a Keithley electrometer (Model 602; Keithley Instruments Co., Cleveland OH). The reported values of V represent the difference in the potential of the subphase surface in the presence and absence of the monolayer.

RESULTS

X-ray Diffraction/Osmotic Stress Measurements. All X-ray diffraction patterns from either DAPC or 1:1 EPC:MOPC preparations contained a broad wide-angle band centered at 4.5 Å and a series of low-angle reflections that indexed as orders of a single lamellar repeat period. These patterns are characteristic of multilamellar liposomes of bilayers in the liquid-crystalline (L_α) phase (Tardieu et al., 1973).

For DAPC bilayers the lamellar repeat period in excess buffer was 64.7 Å, as indicated by the arrow in Figure 1A. The repeat period decreased monotonically with increasing applied pressure (P), reaching a repeat period near 41 Å at the highest applied pressure of 1.6×10^9 dyn/cm^2 ($\log P = 9.2$) (Figure 1A). For 1:1 EPC:MOPC, the lamellar repeat period in excess water was 74.6 Å, as indicated by the arrow

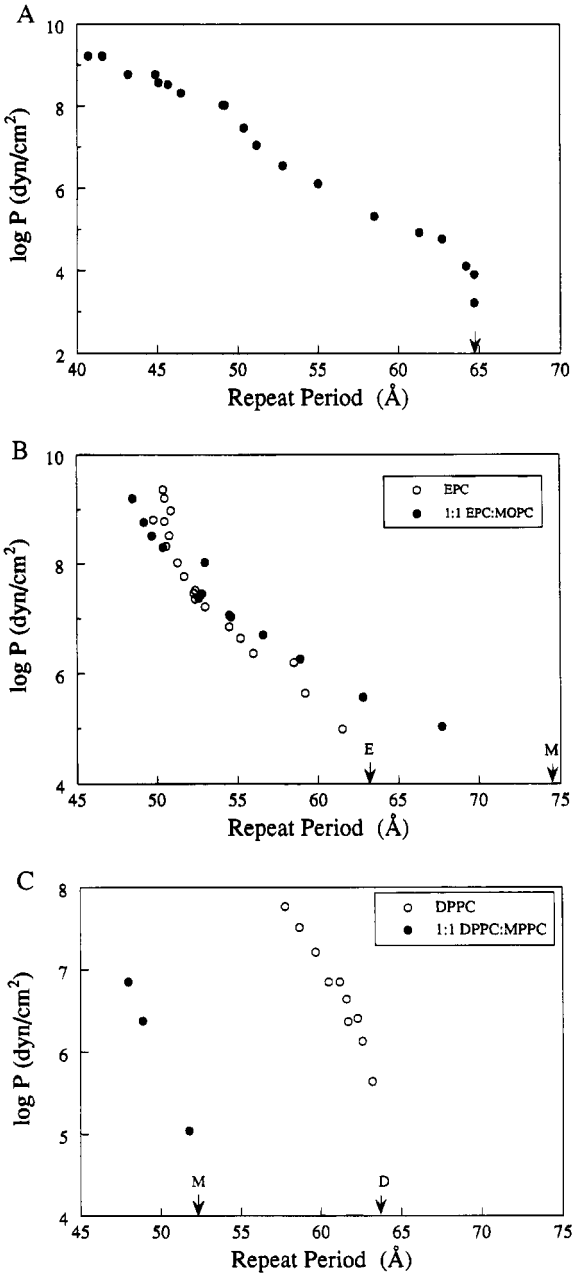

FIGURE 1: Logarithm of applied pressure (log P) plotted versus the lamellar repeat period (d) for (A) DAPC bilayers, (B) EPC bilayers (○) and equimolar EPC:MOPC bilayers (●), and (C) DPPC bilayers (○) and equimolar DPPC:MPPC bilayers (●). In each panel, the repeat periods in excess water with no applied pressure are indicated by arrows, marked E for EPC bilayers, D for DPPC bilayers, and M for both EPC:MOPC and DPPC:MPPC bilayers. Data for EPC and DPPC bilayers are taken from McIntosh and Simon (1986, 1993) and McIntosh et al. (1987).

labelled "M" in Figure 1B. (The same lamellar repeat period was obtained for 1:1 EPC:MOPC in excess 100 mM NaCl and 20 mM HEPES buffer, pH 7.) The value of the lamellar repeat period decreased monotonically with increasing applied pressures (Figure 1B). In Figure 1B, these data are plotted together with previously obtained osmotic stress data for EPC bilayers (McIntosh & Simon, 1986; McIntosh et al., 1987).

For equimolar DPPC:MPPC in excess buffer at 20 °C, the diffraction patterns contained a single sharp wide-angle reflection at 4.09 Å and three low-angle reflections that indexed as the first three orders of a lamellar repeat period of 52.3 Å (indicated by arrow labeled "M" in Figure 1C).

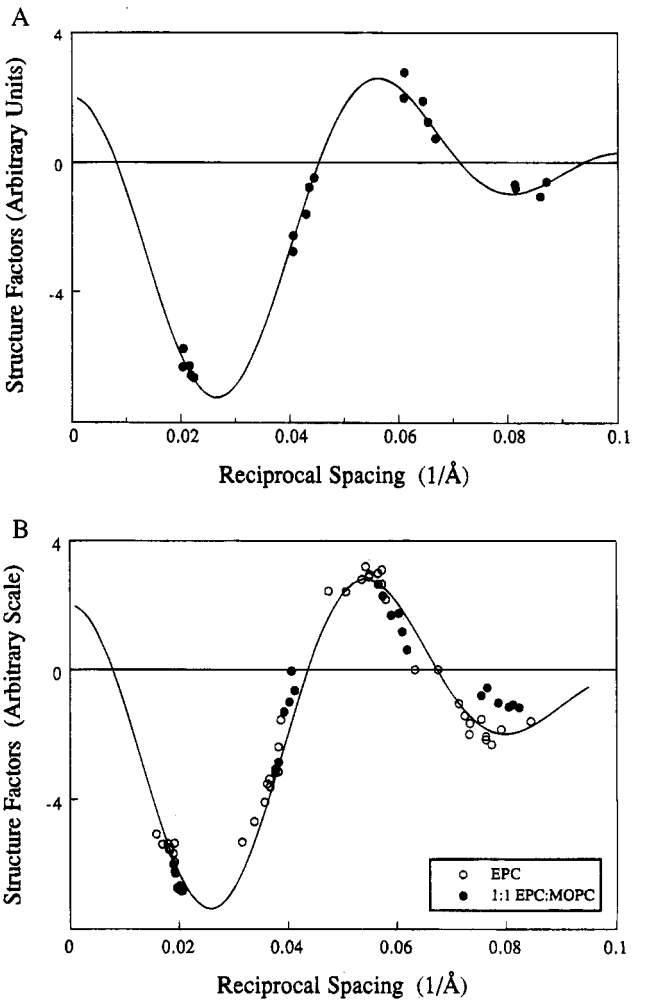

FIGURE 2: Structure amplitudes plotted versus reciprocal space coordinate for (A) DAPC bilayers and (B) EPC (○) and equimolar EPC:MOPC bilayers (●). The lines are continuous transforms calculated from the sampling theorem for DAPC in panel A and EPC in panel B. The data for EPC are taken from McIntosh et al. (1987) and McIntosh and Simon (1986).

Such patterns are typical of multilamellar liposomes containing gel-phase bilayers with the hydrocarbon chains from apposing monolayers fully interdigitated (McIntosh et al., 1983). The repeat period of equimolar DPPC:MPPC bilayers decreased with increasing osmotic pressure, as shown in Figure 1C. For comparison, the diffraction data obtained from DPPC liposomes in the normal, noninterdigitated ($L\beta'$) gel phase are also presented.

The lamellar repeat period includes the total thickness of both the bilayer and the water space between apposing bilayers. To obtain information on the bilayer and fluid layer thicknesses for the data in Figure 1, we performed a Fourier analysis of the diffraction data. Figure 2A shows the structure factors for the lamellar diffraction data from the osmotic stress experiments with DAPC, and Figure 2B shows the structure factors for 1:1 EPC:MOPC, along with the corresponding structure factors for EPC. The phase angles for the EPC diffraction data have previously been determined (McIntosh & Simon, 1986), and the similarity of the relative intensities of the EPC data with both the DAPC and 1:1 EPC:MOPC data (Figure 2A,B) indicates that the same phase angles also pertain to these data sets. For 1:1 DPPC:MPPC the structure factors (data not shown) were very similar to those previously observed for interdigitated DPPC bilayers

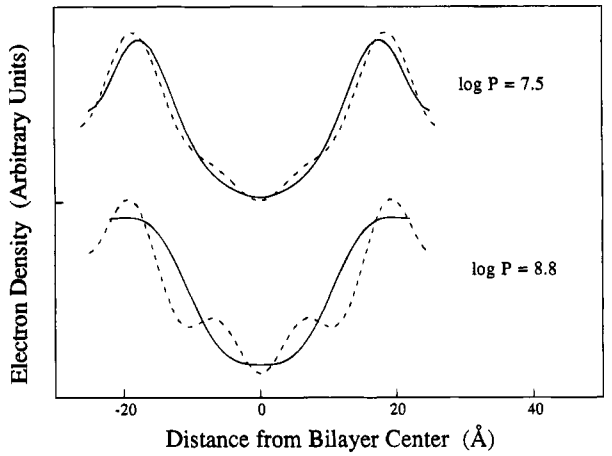

FIGURE 3: Electron density profiles for DAPC (—) and EPC bilayers (- - -) at two values of applied pressure P. Profiles for EPC are taken from McIntosh and Simon (1986).

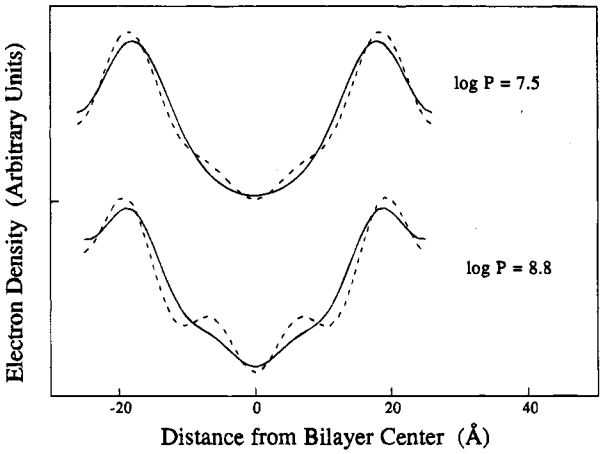

FIGURE 4: Electron density profiles of equimolar EPC:MOPC bilayers (—) and EPC bilayers (- - -) at two values of applied pressure. Profiles for EPC are taken from McIntosh and Simon (1986).

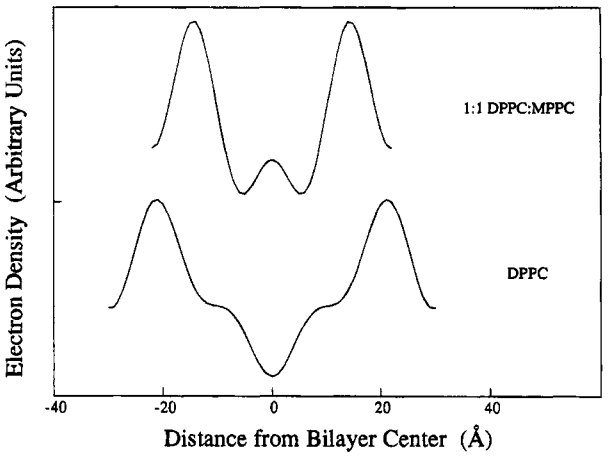

FIGURE 5: Electron density profiles for DPPC bilayers and equimolar DPPC:MPPC bilayers at an applied pressure of 2.8×10^7 dyn/cm^2. The profile for DPPC is taken from McIntosh & Simon (1986).

(McIntosh et al., 1983), and therefore the phase angles were assumed to be the same as those previously determined.

Figure 3 shows electron density profiles for DAPC and, for comparison, EPC bilayers at two osmotic pressures. For each profile, the center of the bilayer is located at 0 Å. The low electron density region in the center of the bilayer corresponds to the lipid hydrocarbon region, and the two electron density peaks, near ±20 Å, correspond to the phospholipid head groups. The medium-density regions at the outer edges of each profile correspond to the fluid spaces between adjacent bilayers. For the smaller applied pressure ($\log P = 7.5$), the profiles for DAPC and EPC were similar in shape, but exhibited two notable differences. First, the distance between head group peaks across the bilayer was smaller for DAPC than for EPC, 34.4 ± 0.7 Å for DAPC and 37.8 ± 0.8 Å for EPC (McIntosh & Simon, 1986). Second, in the case of EPC bilayers, there was a slight dip in the geometric center of the profile corresponding to the localization of terminal methyl groups in the center of the bilayer (McIntosh & Simon, 1986). This terminal methyl trough was absent in the DAPC profile, meaning that the terminal methyl groups were not, on average, as well localized in the geometric center of the bilayer as they were in EPC bilayers. That is, the bilayer interior was more disordered for DAPC than for EPC. For the higher osmotic pressure ($\log P = 8.8$) there was an additional difference between the EPC and DAPC profiles. For EPC there was a medium-density region at the outer edge of the profile, whereas this medium-density region was not present for DAPC bilayers. Thus, for DAPC bilayers subjected to this high applied pressure, the high-density head group peaks from apposing bilayers merged. This same phenomenon has been previously observed in equimolar EPC:cholesterol bilayers (McIntosh et al., 1989a) and indicates that, for large applied pressures, the head group peaks from apposing bilayers have interpenetrated. The difference in appearance of the DAPC and EPC profiles is not due to differences in resolution, since all of the profiles were calculated at the same resolution, $d/2h_{max} = 7$ Å.

Figure 4 shows electron density profiles for EPC and 1:1 EPC:MOPC bilayers at two osmotic pressures. The profiles for EPC and 1:1 EPC:MOPC were similar in shape. However, the distance between head group peaks across the bilayer was about 2 Å larger for EPC than for 1:1 EPC:MOPC, and the terminal methyl trough was absent in the EPC:MOPC profile, indicating more disorder in the hydrocarbon interior. The profiles also show that there was no interpretation of apposing head groups in the case of 1:1 EPC:MOPC, even at applied pressures of $\log P = 8.8$.

Figure 5 shows electron density profiles for DPPC and 1:1 DPPC:MPPC. Again, for each profile, the center of the bilayer is localized at 0 Å, and the high-density peaks correspond to the lipid head groups. The profile for DPPC had a sharp, distinct trough in the center of the bilayer, reflecting the localization of terminal methyl groups in the center of the bilayer. The distance between head group peaks (42 Å) was consistent with the expected width of the bilayer for the normal tilted ($L\beta'$) phase (McIntosh, 1980; McIntosh & Simon, 1986). The profile for 1:1 DPPC:MPPC had several distinct features. First, there was no terminal methyl trough in the center of the bilayers. Second, the distance between head group peaks across the bilayers was only 30 Å. These features, along with the wide-angle diffraction, are characteristic of bilayers in the interdigitated phase, where the hydrocarbon chains from apposing monolayers of the bilayer fully interpenetrate or interdigitate across the bilayer midplane (Ranck et al., 1977; McIntosh et al., 1983; Mattai et al., 1987).

These electron density profiles can be used to estimate the width of the fluid space between bilayers for each applied pressure. As noted previously (McIntosh & Simon, 1986, 1993; McIntosh et al., 1992)), the definition of the lipid/water interface is somewhat arbitrary, because the bilayer surface is not smooth and water penetrates into the head group region of the bilayer (Griffith et al., 1974; Worcester & Franks, 1976; Simon & McIntosh, 1986; Wiener et al., 1991). We operationally define the bilayer width as the total physical thickness of the bilayer, assuming that the conformation of the phosphorylcholine head group in DAPC, EPC, and DPPC bilayers is the same as it is in single crystals of phosphatidylcholine (Pearson & Pascher, 1979). In that case the high-density head group peak would be located between the phosphate group and the glycerol backbone. We assume that the phosphorylcholine group is, on average, oriented approximately parallel to the bilayer plane, so that the edge of the bilayer lies about 5 Å outward from the center of the high-density peaks in the electron density profiles (McIntosh & Simon, 1986, 1993). Therefore, for each osmotic pressure (P) we calculate the bilayer thickness as the distance between head group peaks across the bilayer in the profiles plus 10 Å. The distance between bilayer surfaces (d_f) is calculated as the difference between the lamellar repeat period and this bilayer thickness (McIntosh & Simon, 1986, 1993; McIntosh et al., 1992).

Using this defintion of the lipid/water interface, we plot log P versus d_f for EPC and DAPC in Figure 6A, EPC and 1:1 EPC:MOPC in Figure 6B, and DPPC and 1:1 DPPC:MPPC bilayers in Figure 6C. Several features should be noted about these pressure−distance data. For $d_f < 5$ Å, the incorporation of equimolar MOPC into EPC bilayers had little effect on the pressure−distance relation (Figure 6B), whereas the pressure−distance curve was quite different for DAPC bilayers for this short distance range (Figure 6A). In particular, the application of high pressures (log $P > 8$) reduced the distance between DAPC by about 5 Å compared to EPC bilayers, so that the distance between DAPC bilayers was negative on our distance scale. This implies that for DAPC, but not for the EPC or 1:1 EPC:MOPC bilayers, the head groups from apposing bilayers interpenetrated past our plane of origin, consistent with the merging of the head group peaks in profiles of DAPC at high applied pressures (Figure 3). At longer bilayer separations ($d_f > 5$ Å), each plot of log P versus d_f could be fit to a straight line as shown in Figure 6A,B, implying that the total pressure decrased approximately exponentially with increasing fluid spacing. DAPC and EPC had similar pressure−distance relations for $5 < d_f < 12$ Å and similar exponential decay lengths for the total pressure, 1.8 and 1.7 Å, respectively (Figure 6A). However, the equilibrium fluid separation was about 5 Å larger for DAPC (arrows in Figure 6A). For 1:1 EPC:MOPC bilayers, the decay length of the exponential decay was 2.7 Å, and the equilibrium fluid spacing was about 28 Å, or 13 Å larger than for EPC. The magnitudes of these exponential decays (extrapolated to $d_f = 0$) were 4.0×10^8 and 2.6×10^8 dyn/cm^2 for EPC and 1:1 EPC:MOPC bilayers, respectively. Stated differently, the addition of MOPC to EPC markedly increased the range of the total repulsive pressure between adjacent bilayers, but had very little effect on its magnitude.

In the case of gel-phase DPPC bilayers, the equilibrium fluid separations (marked by arrows in Figure 6C), and thus

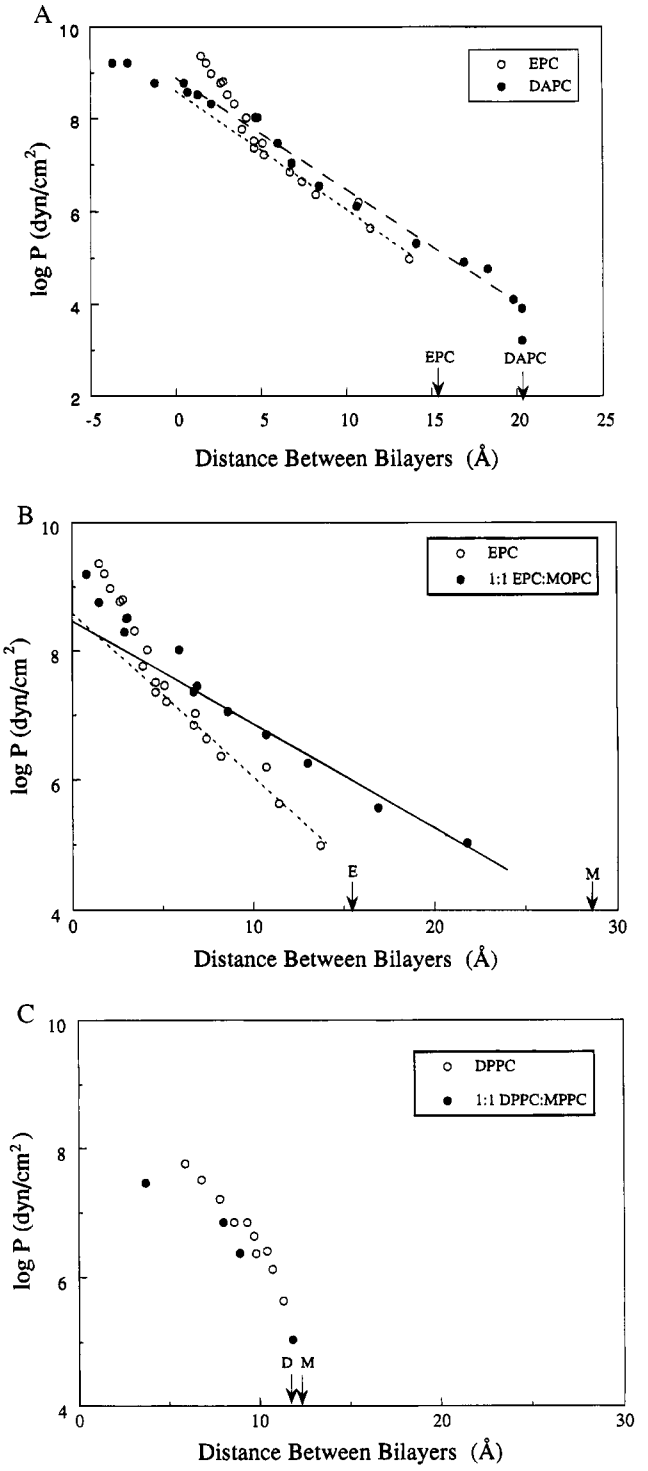

FIGURE 6: Logarithm of applied pressure (log P) plotted versus the distance between bilayers (d_f) for (A) DAPC (●) and EPC bilayers (○), (B) equimolar EPC:MOPC bilayers (●) and EPC bilayers (○), and (C) DPPC (○) and equimolar DPPC:MPPC bilayers (●). In each panel, the distances between bilayers in excess water with no applied pressure are indicated by arrows, marked E for EPC bilayers, D for DPPC bilayers, and M for both EPC:MOPC and DPPC:MPPC bilayers. In panels A and B the straight lines represent least squares fits to the data for $d_f > 5$ Å. The short dashed line (- - -) is the fit to the data for EPC ($P_o = 4.0 \times 10^8$ dyn/cm^2, $\lambda = 1.7$ Å; $R^2 = 0.95$), the long dashed line (— —) is the fit to the DAPC data ($P_o = 7.8 \times 10^8$ dyn/cm^2, $\lambda = 1.8$ Å; $R^2 = 0.98$), and the solid line (—) is the fit to the 1:1 EPC:MOPC data ($P_o = 2.9 \times 10^8$ dyn/cm^2, $\lambda = 2.7$ Å; $R^2 = 0.99$). Data for EPC and DPPC bilayers are taken from McIntosh and Simon (1986, 1993) and McIntosh et al. (1987).

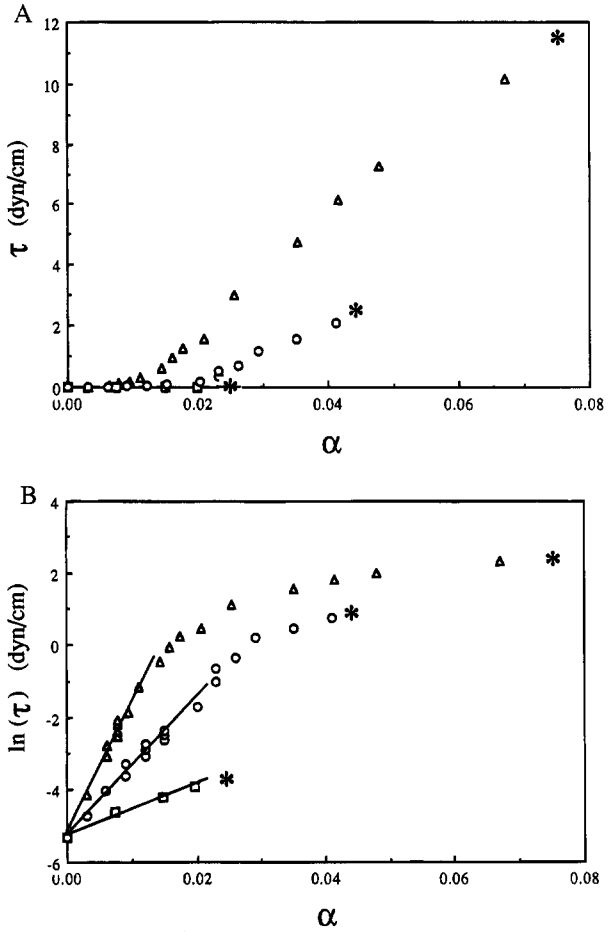

FIGURE 7: Measurements of membrane tension (τ) and fractional area change (α) for EPC (△); DAPC (○); and (1:1) EPC:MOPC (□). (A) Linear scale showing an initial large area increase at low tensions followed by a crossover to a linear high-tension regime at tensions > 1 dyn/cm. The slope in the high-tension regime gives the area expansion modulus. Tensile strengths of the three vesicle compositions are given by the tension at which vesicle lysis occurs as shown by an asterisk (*). (B) Logarithmic plot of the same data showing the fluctuation-dominated low-tension regime. The slope of the exponential dependence gives the bending modulus (see text for details).

the ranges of the total pressure, were nearly the same in the presence and absence of lysophosphatidylcholine.

Dipole Potential Measurements. For DAPC, EPC, and equimolar EPC:MOPC monolayers the dipole potentials were 411.6 ± 12.6 mV (mean ± SD, n = 3 experiments), 408.0 ± 11.5 mV (n = 4), and 379.7 ± 9.6 mV (n = 7), respectively.

Bending Modulus Measurements. Figure 7A shows membrane tension, τ, plotted versus area change, α, and Figure 7B shows ln(τ) plotted versus α, where the area change is taken relative to a reference area measured for membrane tension on the order of 0.005 dyn/cm. In the low-tension regime, the application of very small tensions (<0.5 dyn/cm) caused a fractional increase in the vesicle membrane area (α) of about 0.01 for EPC and about 0.02 for EPC:MOPC and DAPC. EPC and DAPC vesicles then showed a stiffening, and the τ versus α plot became linear with increasing tension up to membrane failure (denoted by * in Figure 7A,B). In contrast, the weaker EPC:MOPC membranes did not show this stiffer slope because they broke in the low-tension regime at 0.019 dyn/cm.

The measured bending moduli (as calculated from eq 5) and the area expansion moduli (as calculated from eq 4) at 14 °C are shown in Table 1. As mentioned earlier, the area expansion modulus for 1:1 EPC:MOPC bilayers could not be measured because the vesicle broke at low tension so that the linear region of the dependence of area change on applied tension was not accessible for measurement (Figure 7A). As also shown in Table 1, the critical tensions for membrane breakdown for EPC and DAPC membranes were found to be 9.4 and 2.1 dyn/cm, respectively, which were well above the threshold of 0.5 dyn/cm for the thermal fluctuation regime. Our measured value for the bending modulus of EPC is similar to the values of 4.0−5.3 × 10^{-13} erg obtained using a different method (Faucon et al., 1989). The value of k_c for DAPC was similar to, but slightly less than, the value of 4.4 × 10^{-13} erg measured at 18 °C by Evans and Rawicz (1990).

DISCUSSION

The data presented here provide information on the effects that polyunsaturation and the incorporation of lysolipids have on the structure of phosphatidylcholine bilayers and on the repulsive pressures between apposing bilayer surfaces.

Structure

DAPC bilayers are 3.4 Å thinner than EPC bilayers (Figure 3), implying that the area per molecule is larger for DAPC than for EPC. To estimate this increase in molecular area, we note that for EPC the hydrocarbon thickness and molecular area are 27.8 Å and 64 Å^2, respectively (McIntosh & Simon, 1986; McIntosh et al., 1989b). Thus the hydrocarbon thickness is about 12% smaller for DAPC than for EPC, and assuming constant densities, we estimate that the molecular area of DAPC should be about 12% larger than that of EPC, or about 73 Å^2. This value is in good agreement with the molecular area of 76 Å^2 found for DAPC monolayers at 30 dyn/cm (Smaby et al., 1994).

The incorporation of equimolar MOPC has a relatively small effect on the structure of liquid-crystalline EPC bilayers, since it decreases the bilayer thickness about 2 Å. In contrast, the incorporation of equimolar MPPC into gel-phase DPPC bilayers has a major structural effect, converting the normal ($L\beta'$) gel phase to an interdigitated gel phase. Previously Van Echteld et al. (1981) have suggested, on the basis of NMR and permeability studies, that lysoPC could induce chain interdigitation in gel-phase DPPC bilayers. Our wide-angle and low-angle X-ray data provide strong evidence that lysoPC does indeed induce an interdigitated phase in gel-phase PC bilayers. In addition, stearoyllysophosphatidylcholine by itself forms an interdigitated bilayer (Hui &

Table 1: Micropipet Measurements

lipid	vesicles measured	bending modulus, k_c (ergs)	area expansion modulus, K_a (dyn/cm)	tensile strength, τ_s (dyn/cm)
EPC	16	(5.06 ± 1.50) × 10^{-13}	167 ± 23	9.36 ± 2.27
DAPC	12	(2.81 ± 0.77) × 10^{-13}	106 ± 23	2.05 ± 0.97
1:1 EPC:MOPC	11	(1.26 ± 0.23) × 10^{-13}	not measurable	0.02 ± 0.01

Huang, 1986) at temperatures below its main acyl chain phase transition.

The structural changes induced by lysophosphatidylcholine in both the gel and liquid-crystalline phases can be rationalized in terms of a model where the monoacyl phosphatidylcholine incorporates into the bilayer with its head group, on average, in the same plane as the head groups of the host bilayers and its hydrocarbon chain oriented in the same direction as the host lipid. Lysophosphatidylcholines have a conical shape, such that in the bilayer plane the lysolipid head group has a larger area than its hydrocarbon chain (Israelachvili et al., 1977; Cullis & DeKruijff, 1979). Thus, when MOPC partitions into the EPC bilayer in the configuration described above, it increases the area in the head group region of the bilayer more than in the hydrocarbon region. To accommodate the conically shaped MOPC molecules and minimize the creation of energetically unfavorable voids, the acyl chains of EPC expand to occupy a larger molecular area. This causes a further disordering of the central region of the bilayers, decreasing the acyl chain thickness and removing the terminal methyl trough usually observed in electron density profiles of more ordered bilayers (see Figure 4). For liquid-crystalline bilayers, the increased area per hydrocarbon chain permits more acyl chain configurations away from the bilayer normal (Baenzinger et al., 1992; Pearce & Harvey, 1993). In the case of gel-phase bilayers, where the chains are comparatively inflexible, the bilayers prevent the formation of potential voids produced by lysophosphatidylcholine by forming a phase where hydrocarbon chains from apposing monolayers fully interdigitate. This interdigitated phase is stabilized by increased van der Waals interactions between hydrocarbon chains compared to those in the Lβ' gel phase (Simon & McIntosh, 1984; Simon et al., 1986).

Interactions between Bilayers

As noted in the introduction, there are several component pressures that are thought to contribute to the total repulsive pressure between electrically neutral PC bilayers, including the hydration pressure and steric pressures due to lipid head group motion, molecular protrusions, and bilayers undulations. We now consider each of these pressures with regard to the above observations on lysophosphatidylcholine-containing bilayers.

Hydration Pressure. The hydration pressure is thought to arise from the orientation or polarization of water by the lipid polar head groups (Cevc & Marsh, 1985; Leikin et al., 1993) or by the head groups reorganizing the H-bond network of water (Attard & Batchelor, 1988). We argue that the hydration pressure cannot be the source of the increased range for the total pressure for DAPC (Figure 6A) and 1:1 EPC:MOPC bilayers (Figure 6B) for several reasons. First, the range of the repulsive pressure for both DAPC (equilibrium fluid separation of 20.3 Å) and EPC:MOPC (equilibrium fluid separation of 28.6 Å) bilayers is beyond the range of the hydration pressure. McIntosh and Simon (1993) have shown that for subgel PC bilayers (where out of plane motions are very small) the range of the hydration pressure is relatively small (equilibrium fluid separation of 9 Å). Second, since DAPC, MOPC, and EPC all have the same head group, the hydration pressure would be expected to be similar for bilayers composed of these molecules. In support of this idea is the observation that the measured dipole potentials for DAPC, EPC, and EPC:MOPC monolayers are similar (within 30 mV). Since the magnitude of the hydration pressure has been shown to be proportional to the square of the dipole potential (Simon & McIntosh, 1989; Simon et al., 1992), the magnitude of the hydration pressure should be similar for DAPC, EPC, and 1:1 EPC:MOPC bilayers. Third, the incorporation of MPPC into gel phase DPPC did not appreciably change the equilibrium fluid space (Figure 6C). If an increase in the hydration pressure were responsible for the large (13.2 Å) increase in equilibrium fluid space when MOPC was added to EPC bilayers, then a corresponding increase would also have been expected with the addition of MPPC to DPPC bilayers.

Steric (Entropic) Pressures Due to Head Group Motion and Lipid Protrusions. Entropic pressures could arise from two types of motions of individual lipid molecules: movement of the lipid head groups and lipid protrusions out of the plane of the bilayer. In the case of liquid-crystalline bilayers these two motions are coupled. In the absence of lipid protrusions, the steric pressure due solely to PC head group motion would extend only to $d_f \approx 5$ Å, corresponding to the maximum extent that a PC head group could extend from the plane of the bilayer (McIntosh et al., 1987). Upward breaks in the pressure−distance relations are observed at $d_f \approx 4-5$ Å for EPC (McIntosh et al., 1987 & 1989a) and 1:1 EPC:MOPC bilayers (Figure 6A,B), but such a break is absent in the pressure−distance curve for DAPC. We argue that the reason for this difference is that the large area per DAPC molecule (approximately 73 Å^2; see above) permits the DAPC head groups from apposing bilayers to interpenetrate at high pressures (Figure 3). This interpretation is in agreement with our previous observations with EPC:cholesterol bilayers (McIntosh et al., 1989a), where the short-range pressure was reduced with increasing area per lipid molecule. That is, the repulsive pressure due to interactions between head groups from apposing bilayers decreases with decreasing volume fraction of head groups at the interface (McIntosh et al., 1989a).

The protrusion pressure was proposed to arise from interactions between individual amphihiles that protrude various extents from apposing monolayers into the aqueous phase. According to Israelachvili & Wennerström (1992), the protrusion pressure P_p can be expressd as

$$P_p = 2.7\, n\alpha \exp(-d_f/\lambda) \qquad (6)$$

where n is the number of protruding molecules per unit area and $\alpha = \pi\sigma\gamma$; σ is the lateral dimension of the protruding molecule, γ is the effective interfacial energy, and λ is the decay length ($\lambda = 1.15kT/\alpha = 1.15kT/\pi\sigma\gamma$). Since σ should be different for amphiphiles with one or two acyl chains, it follows that both the magnitude and the decay length of the protrusion pressure for EPC bilayers should be modified by the addition of MOPC.

To compare the observed pressure−distance relations for EPC and EPC:MOPC bilayers (Figure 6B) to the predictions of the protrusion model, we use eq 6 and make the following simplifying assumptions: (1) the plane of origin for P_p is at the edge of the bilayer ($d_f = 0$), (2) γ is the same for EPC and EPC:MOPC bilayers, and (3) protrusions of MOPC are much more important than protrusions of EPC in EPC:MOPC bilayers. The last assumption is made since the water

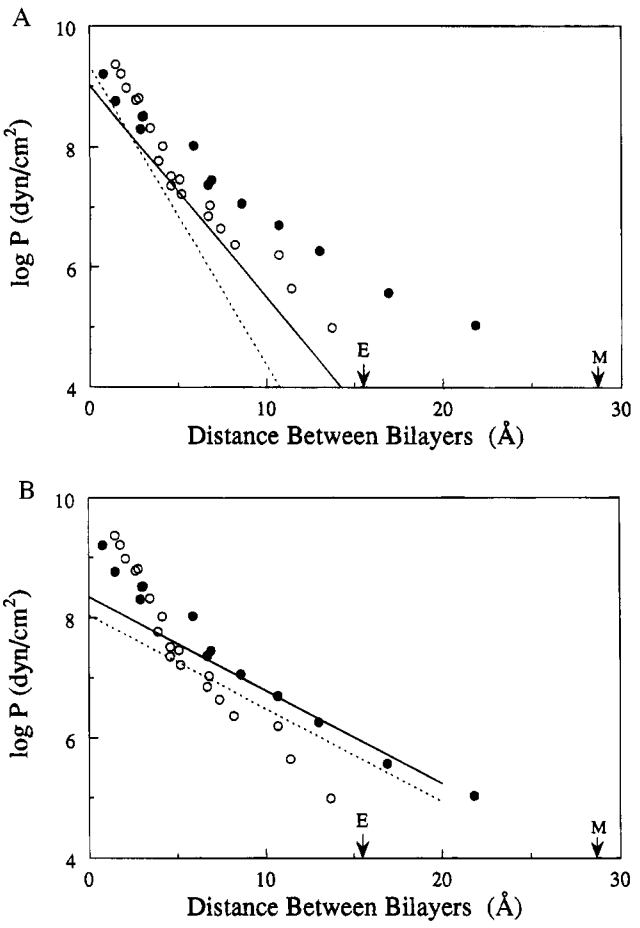

FIGURE 8: Logarithm of applied pressure (log P) plotted versus the distance between bilayers for EPC (○) and equimolar EPC:MOPC bilayers (●) with calculated repulsive pressures (see text for details). In (A) the dotted and solid lines are the protrusion pressures for EPC and EPC:MOPC bilayers, respectively, calculated using eq 6 with $\gamma = 20$ dyn/cm. In (B) the dotted and solid lines represent undulation pressures for EPC and EPC:MOPC bilayers, respectively, calculated using eq 8 and measured values of the bending moduli.

solubility of MOPC is several orders of magnitude larger than the water solubility of EPC (Marsh, 1990). For the EPC bilayers we use the measured area per molecule, $A = 64$ Å^2 (McIntosh et al., 1989b), so that $n = 1/A = 1/64$ Å^2, and for EPC:MOPC bilayers we assume that the area per molecule of MOPC is $A' = 64/2$ Å$^2 = 32$ Å^2, so that $n = 1/(A + A') = 1/96$ Å^2. The values of γ and σ are not known. Israelachvili and Wennerström (1990, 1992) assume that $\gamma = 20$ dyn/cm, whereas Parsegian and Rand (1991) argue that $\gamma = 70$ dyn/cm. To present the protrusion pressure in its most favorable light, we use $\gamma = 20$ dyn/cm. To estimate σ for each hydrocarbon chain, we use the measured value for the energy to expose a CH_2 group to water (E) and the relation that $E = \gamma a$, where a, which is equal to $\pi(\sigma/2)^2$, is the area exposed per CH_2 group. Given that $E = 880$ cal/mol/CH_2 group (Tanford, 1980), we calculate $a = 27.8$ Å^2 and $\sigma = 5.95$ Å. This calculated value of a is somewhat smaller than our estimated value of the area per MOPC molecule ($A' = 32$ Å^2). Therefore, for monoacyl MOPC $\sigma_M = 5.95$ Å, and for diacyl EPC $\sigma_D = (5.95$ Å$)(2)^{1/2} = 8.39$ Å. With these estimated values we calculate the theoretical decay lengths of the protrusion pressure, $\lambda = 1.15kT/\pi\sigma\gamma$, to be 0.87 and 1.23 Å for EPC and EPC:MOPC, respectively. Figure 8A shows plots of these theoretical protrusion pressures for EPC and EPC:MOPC bilayers. For both EPC and 1:1 EPC:MOPC bilayers the calculated protrusion pressures somewhat underestimate the total pressure at small fluid spacings ($d_f < 5$ Å) and greatly underestimate the total observed repulsive pressure at large bilayer separations ($d_f > 5$ Å). Given the uncertainties in the choice of the plane of origin (see above), it appears that, with the above assumptions, the protrusion pressure provides a reasonable prediction for the measured repulsive pressure only at small bilayer separations. That is, a 1−2-Å shift in the plane of origin could provide a fairly close agreement between the data points and the theoretical prediction for $d_f < 5$ Å, but would still leave a significant difference between experiment and theory for $d_f > 5$ Å. It should be noted that letting $\gamma = 70$ dyn/cm would produce poorer agreement with the experimental data.

The theoretical treatment (Israelachvili & Wennerström, 1990, 1992) of the protrusion pressure (eq 6) predicts that λ should be similar for DAPC and EPC and the magnitude of the pressure should be slightly smaller for DAPC than EPC, since the area per molecule is greater for DAPC than for EPC, but the effects of unsaturation on the transfer of hydrocarbon between water and liquid hydrocarbon are relatively small. That is, the surface energies for saturated and unsatruated hydrocarbons do not differ by more than 1−2 dyn/cm (Ried & Sherwood, 1966; Jasper, 1972), and the free energy per carbon to transfer alkanes, alkenes, and alkadienes from hydrocarbon to water is nearly the same (Tanford, 1980). In fact, the observed repulsive pressure is quite different for DAPC and EPC for $d_f < 3$ Å. Thus, the formalism of the protrusion pressure is not sufficiently detailed to predict the changes in the pressure−distance relations produced by the effects of polyunsaturation. We argue, as described above, that lipid head group motion contributes to the total pressure (McIntosh & Simon, 1993) and that, because of their large area per molecule, DAPC head groups for apposing bilayers interpenetrate at large applied pressures.

As noted in the introduction, the analysis for the protrusion pressure (Israelachvili & Wennerström, 1990, 1992) does not explicitly address the behavior of amphiphiles in gel-phase lipids, since it is stated to be applicable for van der Waals liquids (Israelachvili, 1991). We argue that molecular protrusions in a gel-phase bilayer would be small compared to those in a liquid-crystalline phase bilayer, since the free energy necessary to transfer an amphiphile from bilayer to water would be expected to be greater for a gel phase (by the free energy of fusion) than for a liquid-crystalline phase (McIntosh & Simon, 1994). The absence of a significant difference in the equilibrium fluid separation for gel-phase DPPC and DPPC:MPPC bilayers (Figure 6C) is consistent with the presence of an underlying hydration pressure for gel bilayers (Parsegian & Rand, 1991; McIntosh & Simon, 1993, 1994).

Steric Pressure from Bilayer Undulations. The undulation pressure (P_u) is a steric pressure between bilayers due to interactions between thermally induced undulations or fluctuations of the entire bilayer (Helfrich, 1978; Harbich & Helfrich, 1984; Evans & Parsegian, 1986; Evans & Ipsen, 1991). According to Evans and Parsegian (1986), when there is an underlying repulsive pressure (such as an electrostatic or a hydration pressure) between adjacent bilayers with the form

$$P = P_o \exp(-d_f/\lambda) \quad (7)$$

then the undulation pressure in the small fluctuation regime can be written

$$P_u = (\pi kT/32)(P_o/k_c\lambda^3)^{1/2} \exp(-d_f/2\lambda) \quad (8)$$

Note that the decay length of P_u is twice the decay length of the underlying pressure and that the magnitude of P_u is inversely proportional to the square root of the bending modulus, k_c. Interactions between EPC bilayers have been shown to contain contributions from P_u (Evans & Parsegian, 1986; Evans, 1991; McIntosh & Simon, 1993, 1994).

Tests to determine the contribution of the undulation pressure to the total repulsive pressure are somewhat indirect because its magnitude and range depend on the values of P_o and λ for the underlying pressure. For P_o and λ we use 1.1 $\times$ 10^9 dyn/cm^2 and 1.4 Å, respectively, which are values from the repulsive pressure measured between DPPC bilayers in the crystalline subgel phase where undulations are markedly decreased (McIntosh & Simon, 1993). Figure 8B shows plots of the undulation pressure for EPC and 1:1 EPC:MOPC bilayers obtained using eq 8, these values of P_o and λ, and measured values of k_c (Table 1). Comparison of panels A and B of Figure 8 shows that the undulation pressure has a much longer range than the calculated protrusion pressure and gives a reasonable fit to the 1:1 EPC:MOPC data for fluid spacings 8 < d_f < 20 Å. For EPC bilayers, the calculated undulation pressure only approximates the data for 5 < d_f < 8 Å. At larger spacings, P_u overestimates the total repulsive pressure, most likely because the attractive van der Waals pressure was not considered (see below). For fluid spacings < 5 Å, the undulation pressure greatly underestimates the total pressure for both bilayers. This underestimation can be explained by the contributions to the total pressure of other short-range pressures, such as the hydration pressure, the protrusion pressure, and the steric pressure due to head group motion (see above). To account for the increases in equilibrium fluid spacing found with DAPC and by incorporation of MOPC into EPC bilayers, it is necessary to take into account both attractive and repulsive pressures, as we now consider.

Evans (1991) developed a self-consistent field approximation to predict the continuous unbinding of multilamellar liquid-crystalline membranes of various thicknesses as functions of the underlying exponential repulsive pressure, the attractive van der Waals pressure, and the bending modulus. He assumed the van der Waals pressure to have a power law dependence and a magnitude characterized by the Hamaker constant, A_H, and the undulation pressure to be characterized by the Helfrich energy scale, $E_H = (kT)^2/16\pi^2ck_c$, where the parameter $c \approx 0.1$ (Evans, 1991). Values for E_H are given in Table 2. Evans plotted the parameter λ/d_{eq} versus A_H/E_H for different values of the parameter $V_r = P_o\lambda^3/E_H$. Evans (1991) used a definition for the plane of origin of the attractive and repulsive pressures different from ours, as he used the plane of origin obtained from gravimetric analysis of X-ray diffraction data (Tardieu et al., 1973; LeNeveu et al., 1977). From previous comparisons of electron density profiles and gravimetric analysis of EPC bilayers, McIntosh et al. (1989b) found that the fluid spaces calculated using these different planes of origin differ by 7.9 Å (see Table 2). This means that, with the Evans plane of origin, P_o is greater than the one we reported for DPPC in the subgel phase (1.1×10^9 dyn/cm^2) by a factor of {exp-(7.9 Å/1.4 Å)}, and the equilibrium fluid spacings (d_{eq}) on the Evans scale is equivalent to our measured values (Figure 6B) plus 7.9 Å. Using these values, we calculate $V_r \approx 3 \times 10^3$ for EPC bilayers. In subsequent calculations we use the closest published curve, where $V_r = 10^3$ (Figure 9). To predict d_{eq} for DAPC and 1:1 EPC:MOPC bilayers, it is necessary to know A_H for EPC bilayers. This can be estimated by selecting the A_H/E_H value corresponding to λ/d_{eq} = 1.4 Å/23.3 Å = 0.06 for EPC (see Figure 9). This gives $A_H/E_H = 420$, so that $A_H = 8.6 \times 10^{-14}$ erg, a very reasonable value (Evans, 1991). Because DAPC and MOPC both have the same head group, it is reasonable to assume that both DAPC and 1:1 EPC:MOPC bilayers have similar values of A_H (Mahanty & Ninham, 1976; Israelachvili, 1991). The small changes in d_{eq} found in DPPC and DPPC:MPPC bilayers (Figure 6C) are additional evidence for assuming that the incorporation of lysophosphatidylcholine does not appreciably change A_H. Using the values of E_H given in Table 2, we find from the curve in Figure 9 that d_{eq} = 30.1 Å for DAPC and 48.3 Å for 1:1 EPC:MOPC (Table 2). These values are larger than the measured values by 2 and 12 Å, respectively (Table 2). The agreement between theory and experiment is very good for DAPC bilayers. Considering the large experimental uncertainty in k_c and the many assumptions involved in the calculations, we argue that the agreement between experiment and theory is reasonable for MOPC:EPC. Thus, the Evans (1991) theory predicts that undulations can account for the relatively large equilibrium

Table 2: Equilibrium Fluid Spacings Measured and Calculated from Undulation Theory (Evans, 1991)

lipid	E_H (erg)	d_{eq} (Fourier) (Å)	d_{eq} (gravimetric) (Å)	d_{eq} (calculated) (Å)
EPC	2.00×10^{-16}	15.4	23.3	23.3
DAPC	3.61×10^{-16}	20.3	28.2	30.1
1:1 EPC:MOPC	8.05×10^{-16}	28.6	36.5	48.3

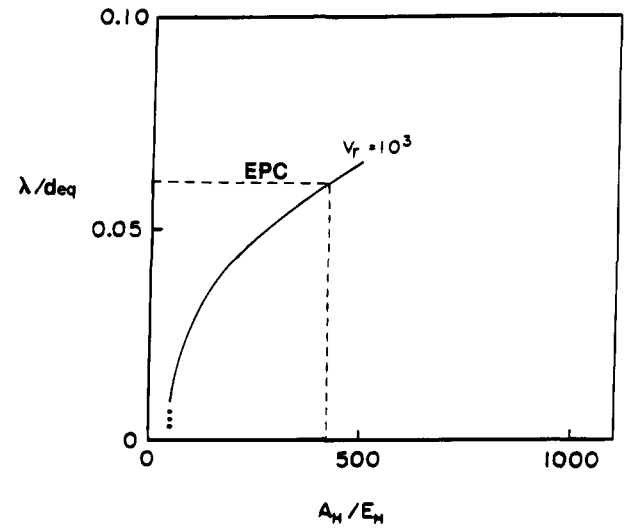

FIGURE 9: Plot of λ/d_{eq} versus A_H/E_H, where λ is the decay length of the underlying repulsive pressure, d_{eq} is the observed fluid spacing in excess water using the Evans scale, A_H is the Hamaker constant, and E_H is the Helfrich energy scale (see text for details.) Values for EPC are shown by the dashed lines. This plot is redrawn from Figure 7 of Evans 1991).

fluid spaces for both DAPC and 1:1 EPC:MOPC. As shown in Figure 8B, undulations should also enhance the repulsive interaction over an extended range of d_f below the equilibrium fluid separation.

Although one cannot quantitate the undulation pressure for gel-phase bilayers since the bending modulus of defect-free bilayers is too small to be measured, one would expect that the undulation pressure would be extremely small for gel-phase bilayers. Thus, at least qualitatively, the relatively small equilibrium fluid separation for both DPPC and 1:1 DPPC:MPPC can be explained by the balance between van der Waals attraction and a short-range hydration pressure (McIntosh & Simon, 1993).

Thus, the equilibrium fluid spacing observed for DAPC bilayers can be closely predicted by the effects of bilayer undulations on an underlying short-range repulsive pressure. Similarly, the increase in repulsive pressure resulting from the incorporation of MOPC into EPC bilayers can be accounted for by an increased undulation pressure. Molecular protrusions appear to contribute appreciably to the repulsive pressure between bilayers only at small fluid spacings.

Finally, the effects of lysophosphatidylcholine on the undulation pressure may help to explain why exogenous lysolipids inhibit membrane fusion. It has been found that the addition of lysophosphatidylcholine reversibly blocks exocytosis and viral fusion (Vogel et al., 1993) and fusion between several types of biological membranes (Chernomordik et al., 1993). The mechanism of this lysolipid inhibition of fusion is unclear (Vogel et al., 1993), and we suggest that it may be due, at least in part, to a lysolipid-induced increase in bilayer undulations and the resultant increase in the repulsive pressure between membranes.

ACKNOWLEDGMENT

We thank Drs. M. Berkowitz, E. A. Evans, and J. I. Israelachvili for helpful discussions during the course of this work.

REFERENCES

Attard, P., & Batchelor, M. T. (1988) *Chem. Phys. Lett. 149*, 206–211.
Baenzinger, J. E., Jarrell, H. C., & Smith, I. C. P. (1992) *Biochemistry 31*, 3377–3385.
Blaurock, A. E., & Worthington, C. R. (1966) *Biophys. J. 6*, 305–312.
Cevc, G., & Marsh, D. (1985) *Biophys. J. 47*, 21–32.
Chernomordik, L. V., Vogel, S. S., Sokoloff, A., Onaran, H. O., Leikina, E. A., & Zimmerberg, J. (1993) *FEBS Lett. 318*, 71–76.
Cullis, P. R., & DeKruijff, B. (1979) *Biochim. Biophys. Acta 559*, 399–420.
Damodaran, K. V., & Merz, K. M., Jr. (1994) *Biophys. J. 66*, 1076–1087.
Elamrani, K., & Blume, A. (1982) *Biochemistry 21*, 521–526.
Evans, E. (1991) *Langmuir 7*, 1900–1908.
Evans, E. A., & Skalak, R. (1980) *Mechanics and Thermodynamics of Biomembranes*, CRC Press, Boca Raton, FL.
Evans, E. A., & Parsegian, V. A. (1986) *Proc. Natl. Acad. Sci. U.S.A. 83*, 7132–7136.
Evans, E. A., & Rawicz, W. (1990) *Phys. Rev. Lett. 64*, 2094–2097.
Evans, E., & Ipsen, J. (1991) *Electrochim. Acta 36*, 1735–1741.
Faucon, J. F., Mitov, M. D., Meleard, P., Bivas, I., & Bothorel, P. (1989) *J. Phys. (Paris) 50*, 2389–2414.
Griffith, O. H., Dehlinger, P. J., & Van, S. P. (1974) *J. Membr. Biol. 15*, 159–192.
Harbich, W., & Helfrich, W. (1984) *Chem. Phys. Lipids 36*, 39–63.
Helfrich, W. (1978) *Z. Naturforsch. 33A*, 305–315.
Heller, H., Schaefer, M., & Schulten, K. (1993) *J. Phys. Chem. 97*, 8343–8360.
Herbette, L., Marquardt, J., Scarpa, A., & Blasie, J. K. (1977) *Biophys. J. 20*, 245–272.
Hui, S. W., & Huang, C.-h. (1986) *Biochemistry 25*, 1330–1334.
Israelachvili, J. N. (1991) *Intermolecular and Surface Forces*, Academic Press, London.
Israelachvili, J. (1992) *Langmuir 8*, 1501.
Israelachvili, J. N., & Wennerström, H. (1990) *Langmuir 6*, 873–876.
Israelachvili, J. N., & Wennerström, H. (1992) *J. Phys. Chem. 96*, 520–531.
Israelachvili, J. N., Mitchell, J., & Ninham, B. W. (1977)) *Biochim. Biophys. Acta 470*, 185–201.
Jasper, J. J. (1972) *J. Phys. Chem. Ref. Data 1*, 841–1010.
Konig, S., Pfeiffer, W., Richter, D., Bayerl, T., & Sackmann, E. (1992) *J. Phys. 2*, 1589–1594.
Kwok, R., & Evans, E. (1981) *Biophys. J. 35*, 637–652.
Leikin, S., Parsegian, V. A., & Rau, D. C. (1993) *Annu. Rev. Phys. Chem. 44*, 369–395.
LeNeveu, D. M., Rand, R. P., Parsegian, V. A., & Gingell, D. (1977) *Biophys. J. 18*, 209–230.
Lipowsky, R., & Grotehans, S. (1993) *Europhys. Lett. 23*, 599–604.
Lipowsky, R., & Grotehans, S. (1994) *Biophys. Chem. 49*, 27–37.
MacDonald, R. C., & Simon, S. A. (1987) *Proc. Natl. Acad. Sci. U.S.A. 84*, 4089–4094.
MacDonald, R. I. (1985) *Biochemistry 24*, 4058–4066.
Mahanty, J., & Ninham, B. W. (1976) *Dispersion Forces*, Academic Press, New York.
Marcelja, S., & Radic, N. (1976) *Chem. Phys. Lett. 42*, 129–130.
Marrink, S.-J., Berkowitz, M., & Berendsen, H. J. C. (1993) *Langmuir 9*, 3122–3131.
Marsh, D. (1990) *Handbook of Lipid Bilayers*, pp 275–280, CRC Press, Boca Raton, FL.
Mattai, J., Witzke, N. M., Bittman, R., & Shipley, G. G. (1987) *Biochemistry 26*, 623–633.
McIntosh, T. J. (1980) *Biophys. J. 29*, 237–246.
McIntosh, T. J., & Simon, S. A. (1986) *Biochemistry 25*, 4058–4066.
McIntosh, T. J., & Holloway, P. W. (1987) *Biochemistry 26*, 1783–1788.
McIntosh, T. J., & Simon, S. A. (1993) *Biochemistry 32*, 8374–8384.
McIntosh, T. J., & Simon, S. A. (1994) *Annu. Rev. Biophys. Biomol. Struct. 23*, 27–51.
McIntosh, T. J., McDaniel, R. V., & Simon, S. A. (1983) *Biochim. Biophys. Acta 731*, 109–114.
McIntosh, T. J., Magid, A. D., & Simon, S. A. (1987) *Biochemistry 26*, 7325–7332.
McIntosh, T. J., Magid, A. D., & Simon, S. A. (1989a) *Biochemistry 28*, 17–25.
McIntosh, T. J., Magid, A. D., & Simon, S. A. (1989b) *Biochemistry 28*, 7904–7912.
McIntosh, T. J., Magid, A. D., & Simon, S. A. (1989c) *Biophys. J. 55*, 897–904.
McIntosh, T. J., Simon, S. A., Needham, D., & Huang, C.-h. (1992) *Biochemistry 31*, 2020–2024.
Needham, D., & Evans, E. (1988) *Biochemistry 27*, 8261–8269.
Needham, D., & Nunn, R. S. (1990) *Biophys. J. 58*, 997–1009.
Needham, D., & Zhelev, D. V. (1995) *Ann. Biomed. Eng.* (in press).
O'Brien, F. E. M. (1948) *J. Sci. Instrum. 25*, 73–76.
Parsegian, V. A., & Rand, R. P. (1991) *Langmuir 7*, 1299–1301.
Parsegian, V. A., & Rand, R. P. (1992) *Langmuir 8*, 1502.
Parsegian, V. A., Fuller, N., & Rand, R. P. (1979) *Proc. Natl. Acad. Sci. U.S.A. 76*, 2750–2754.
Parsegian, V. A., Rand, R. P., Fuller, N. L., & Rau, R. C. (1986) *Methods Enzymol. 127*, 400–416.
Pearce, L. L., & Harvey, S. C. (1993) *Biophys. J. 65*, 1084–1092.
Pearson, R. H., & Pascher, I. (1979)) *Nature 281*, 499–501.

Pfeiffer, W., Henke, T., Sackmann, E., Knoll, W., & Richter, D. (1989) *Europhys. Lett. 8*, 201−206.
Pfeiffer, W., Konig, S., Legrand, J. F., Bayerl, T., Richter, D., & Sackmann, E. (1993) *Europhys. Lett. 23*, 457−462.
Podgornik, R., & Parsegian, V. A. (1992) *Langmuir 8*, 557−562.
Ranck, J. L., Keira, T., & Luzzati, V. (1977) *Biochim. Biophys. Acta 488*, 432−441.
Rand, R. P., & Parsegian, V. A. (1989) *Biochim. Biophys. Acta 988*, 351−376.
Ried, R. C., & Sherwood, T. K. (1966) *The Properties of Gases and Liquids, 2nd ed.*, McGraw Hill Book Co., New York.
Roux, D., & Safinya, C. R. (1988) *J. Phys. (Paris) 49*, 307−318.
Safinya, C. R. (1989) in *Phase Transitions in Soft Condensed Matter* (Riste, T., & D. Sherrington, D., Eds.) pp 249−270, Plenum Publishing Corp., New York.
Safinya, C. R., Roux, D., Smith, G. S., Sinha, S. K., Dimon, P., Clark, N. A., & Bellocq, A. M. (1986) *Phys. Rev. Let. 57*, 2718−2721.
Shannon, C. E. (1949) *Proc. Inst. Radio Eng. N.Y. 37*, 10−21.
Simon, S. A., & McIntosh, T. J. (1984) *Biochim. Biophys. Acta 773*, 169−172.
Simon, S. A., & McIntosh, T. J. (1986) *Methods Enzymol. 127*, 511−521.
Simon, S. A., & McIntosh, T. J. (1989) *Proc. Natl. Acad. Sci. U.S.A. 86*, 9263−9267.
Simon, S. A., McIntosh, T. J., & Hines, M. L. (1986) in *Molecular and Cellular Mechanisms of Anesthetics* (Roth, S. H., Miller, K., Eds.) pp 297−308, Plenum Publishing Co., New York.
Simon, S. A., McIntosh, T. J., Magid, A. D., & Needham, D. (1992) *Biophys. J. 61*, 786−799.
Smaby, J. M., Brockman, H. L., & Brown, R. E. (1994) *Biochemistry 33*, 9135−9142.
Tanford, C. (1980) *The Hydrophobic Effect*, pp 5−13, John-Wiley & Sons, New York.
Tardieu, A., Luzzati, V., & Reman, F. C. (1973) *J. Mol. Biol. 75*, 711−733.
Van Echteld, C. J. A., DeKruijff, B., Mandersloot, J. G., & DeGier, J. (1981) *Biochim. Biophys. Acta 649*, 211−220.
Vogel, S. S., Leikina, E. A., & Chernomordik, L. V. (1993) *J. Biol. Chem. 268*, 25764−25768.
Weast, R. C. (1984) *Handbook of Chemistry and Physics*, CRC Press, Boca Raton, FL.
Wiener, M. C., King, G. I., & White, S. H. (1991) *Biophys. J. 60*, 568−576.
Wimley, W. C., & Thompson, T. E. (1991) *Biochemistry 30*, 1702−1709.
Worcester, D. L., & Franks, N. P. (1976) *J. Mol. Biol. 100*, 359−378.
Wu, J. R., & Lentz, B. R. (1991) *Biochemistry 30*, 6780−6787.
Zhelev, D. V., Needham, D., & Hochmuth, R. M. (1994) *Biophys. J, 67*, 720−727.

BI950362X